International Journal of Mass Spectrometry 306 (2011) 70–76

Contents lists available at ScienceDirect

International Journal of Mass Spectrometry

journal homepage: www.elsevier.com/locate/ijms

Dissociation characteristics of α,ω-dihydride poly(dimethylsiloxane) ammonium adducts generated by electrospray ionization

Thierry Fouquet[a,b], Stéphane Humbel[c], Laurence Charles[a,*]

[a] Universités Aix-Marseille I, II & III – CNRS, UMR 6264: Laboratoire Chimie Provence, Spectrométries Appliquées à la Chimie Structurale, F-13397 Marseille Cedex 20, France
[b] Department of Advanced Materials and Structures, Centre de Recherche Public Henri Tudor (CRPHT), Rue de Luxembourg 66, L-4002 Esch sur Alzette, Luxembourg
[c] Aix-Marseille Université – CNRS, UMR 6263: Institut des Sciences Moléculaires de Marseille, Chimie Théorique et Mécanismes, F-13397 Marseille Cedex 20, France

ARTICLE INFO

Article history:
Received 11 May 2011
Received in revised form 27 June 2011
Accepted 27 June 2011
Available online 2 July 2011

Keywords:
PDMS
Tandem mass spectrometry
Hydride terminations
Synthetic polymer
Ammonium adducts

ABSTRACT

Dissociation behavior of ammonium adducts of α,ω-dihydride poly(dimethylsiloxane) (H-PDMS) produced by electrospray ionization was studied in collisional activation conditions. In contrast to MS/MS spectra of synthetic polymers usually displaying fragment series on the whole *m/z* range, ammonium adducts of H-PDMS were shown to always generate the same product ions regardless of the size of the precursor ion. Based on accurate mass measurement and *ab initio* calculation, mechanisms could be proposed to account for this MS/MS pattern. A primary reaction consisting of release of ammonia and hydrogen from activated oligomer adducts would be rapidly followed by elimination of a three dimethylsiloxane-containing cyclic species to generate the three main product ions at *m/z* 207, 281 and 355. Further dissociation of these three species would explain additional signals in MS/MS spectra. Although a similar behavior was previously observed for PDMS bearing methyl terminations (CH_3-PDMS), strong variations in product ion relative abundance were measured as the size of oligomeric precursor increased in the case of H-PDMS. Perfect similarity of MS/MS spectra is shown to occur once hydride end-groups are no longer involved in primary dissociation reactions. Measuring the degree of similarity between MS/MS spectra of consecutive oligomers within PDMS distribution indicates a much higher reactivity of hydride terminations towards the adducted ammonium cation, as compared to methyl end-groups.

1. Introduction

Tandem mass spectrometry (MS/MS) is increasingly applied in the field of synthetic polymers to individually mass-characterize chain terminations. Upon collisional activation, intact oligomer adducts produced by electrospray ionization (ESI) or matrix-assisted laser desorption/ionization (MALDI) usually dissociate via reactions involving backbone cleavages, so-formed product ions hence containing either the initiating or the terminating moiety. A typical fragmentation behavior can thus be defined for a given type of synthetic polymers, and used as a reference to characterize unknowns within the same class. Fragmentation pathways of most common synthetic polymers submitted to collision-induced dissociation (CID) have recently been reviewed by Wesdemiotis et al. [1]. Dissociation pattern might however differ from established rules in case of polymers bearing labile end-groups, such as those obtained in controlled radical polymerization [2]. For example, the main dissociation route of poly(ethylene oxide) (PEO) oligomers adducted with lithium was observed to proceed via the homolytic cleavage of a C–ON bond within the ω group [3], aimed at undergoing reversible homolysis during nitroxide mediated polymerization [4]. This dominant mechanism was shown to efficiently compete with structurally informative CID reactions usually reported for PEO [5–10].

End-groups can also significantly influence in-chain bond cleavages of synthetic polymers, as shown for cationized poly(dimethylsiloxane) (PDMS), preventing any general rules to be established. Using lithium as the cationizing agent in ESI, trimethylsilyl-terminated PDMS oligomers were reported to expel only one monomer unit [11] while CID of α,ω-dihydroxy PDMS was shown to give rise to two major product ion distributions after in-chain cleavages [1]. Chen has proposed that the presence of labile hydrogen atoms in the end-group may play an important role in the dissociation of siloxane bonds [12]. Alternatively, backbiting mechanisms were shown to be involved in CID of PDMS bearing nucleophilic end-groups, such as α,ω-bis(3-aminopropyl)-PDMS [12,13]. In addition, Mayer et al. have reported that dissociation of trimethylsilyl-terminated PDMS (CH_3-PDMS) was also influenced by the nature of the adducted cation [11]. CID of $[PDMS + Li]^+$ was shown to consist of release of one DMS unit, either as a neutral or as a lithiated molecule, whereas a bare metal ion was the only product generated upon activation of sodium or potassium

* Corresponding author. Tel.: +33 491 28 8678; fax: +33 491 28 2897.
E-mail address: laurence.charles@univ-provence.fr (L. Charles).

1387-3806/$ – see front matter © 2011 Elsevier B.V. All rights reserved.
doi:10.1016/j.ijms.2011.06.020

adducts. In contrast, two series of low abundance ions could be observed in CID spectra of silver adducts, assigned to linear and cyclic fragments formed in a process involving a four-member siloxane ring [11]. Very different results were obtained while activating ammonium adducts of CH_3-PDMS: three main ions at m/z 221, m/z 295 and m/z 369, were produced, regardless of the number of monomer units in the precursor ion [14]. Based on *ab initio* calculation, a cyclic structure was assigned to these three product ions, involving as many DMS units as possible and a trimethylsilyl group substituent on the positively charged oxygen. Their formation could be rationalized according to backbiting reactions. Involvement of methyl end-groups in the observed dissociation pathways was mainly demonstrated for the smallest precursor ions ($n < 7$). Release of methane, together with ammonia, would exclusively arise from protonation of an end-of-chain methyl group, producing ions carrying a positive charge on an end-of-chain silicon atom. These primary product ions would then undergo a backbiting reaction to release cyclic PDMS neutrals of different size to produce one of the three most stable cyclic ions at m/z 221, m/z 295 and m/z 369. However, although proceeding through an alternative mechanism with no role of the methyl end-groups, CID of largest precursor ions gave rise to the same MS/MS pattern.

To find out whether the peculiar dissociative behavior of PDMS could be affected by the polymer terminations, unimolecular fragmentation of hydride-terminated PDMS electrosprayed as ammonium adducts was studied in CID conditions.

2. Experimental

2.1. Chemicals

Methanol was purchased from SDS (Peypin, France) while tetrahydrofuran (THF) was from Riëdel-de Haen (Seelze, Germany). Hydride-terminated poly(dimethylsiloxane) (M_n 590 g mol^{-1}) and ammonium acetate was from Sigma Aldrich (St. Louis, MO). PDMS polymer was first dissolved in THF and further diluted using methanolic salt (3 mM) solution to a final 10 μg mL^{-1} concentration.

2.2. Mass spectrometry

High resolution MS and MS/MS experiments were performed using a QStar Elite mass spectrometer (Applied Biosystems SCIEX, Concord, ON, Canada) equipped with an electrospray ionization source operated in the positive mode. The capillary voltage was set at +5500 V and the cone voltage at +50 V. In this hybrid instrument, ions were measured using an orthogonal acceleration time-of-flight (oa-TOF) mass analyzer. A quadrupole was used for selection of precursor ions to be further submitted to collision-induced dissociation (CID) in MS/MS experiments. In MS, accurate mass measurements were performed using two reference ions from a poly(ethylene glycol) internal standard, according to a procedure described elsewhere [15]. The precursor ion was used as the reference for accurate measurements of product ions in MS/MS spectra. MS^3 experiments were performed using a 3200 Q-TRAP mass spectrometer (Applied Biosystems SCIEX), equipped with an electrospray ionization source operated in the positive mode. The capillary voltage was set at +5500 V and the cone voltage at +50 V. Primary precursor ions generated in the ion source were selected in the quadrupole analyzer and submitted to CID in a collision cell. Secondary precursor ions produced during collisions were selected and then fragmented in a linear ion trap. In both instruments, air was used as the nebulizing gas (10 psi) while nitrogen was used as the curtain gas (20 psi) as well as the collision gas. Collision energy was set according to the experiments. Instrument control, data acquisition and data processing of all experiments were achieved using Analyst software (QS 2.0 and 1.4.1 for the QqTOF and the QqTrap instruments, respectively) provided by Applied Biosystems. Sample solutions were introduced in the ionization source at a 5 μL min^{-1} flow rate using a syringe pump.

2.3. Computational details

Geometry optimizations were performed using the hybrid B3LYP density functional theory (DFT) approach as implemented in Gaussian 03 [16]. The functional includes the three parameter Becke exchange functional [17] and the LYP correlation functional [18]. This type of approach is reputedly robust against the choice of the basis set [19], although in some instances differences have been documented [20,21]. We used here the extended 6-311g(2d,p) basis set [22,23], which is adequately large, so basis set superposition error should be small in the computed dissociations, and brings two sets of polarization function for the heavy atoms. This B3LYP/6-311G(2d,p) level of calculation is very similar to the B3LYP/6-311+G(2d,p) level which has been recommended for accurate energetic consideration of atomization [24]. It is likely to offer an accurate description in the fragmentations pathway of the cations studied here.

3. Results and discussion

3.1. ESI-MS/MS of hydride-terminated PDMS ammonium adducts

The ESI mass spectrum of α,ω-dihydride linear PDMS (further noted H-PDMS) shows an intense distribution of singly charged PDMS ammonium adducts with n ranging from 4 to 25, the highest congeners ($n > 19$) being of very low abundance (Supplementary Fig. S1). Calculated value obtained for the number average molecular mass using these MS data was found to be 628 Da, which is consistent with the M_n value of 590 Da announced by the supplier. Apart from this main distribution, a secondary oligomeric ion series displaying peaks spaced by 74 Da could also be detected with low intensity. Even m/z values of these singly charged molecules indicate this second PDMS polymer has also been ionized as ammonium adducts and the sum of the end-group masses, $m_\alpha + m_\omega = 76$ Da, would suggest a partially hydrolyzed PDMS polymer, as previously reported in α,ω-dihydride linear PDMS samples [25].

MS/MS experiments were performed for different ions from the main distribution and, as previously shown for CH_3-PDMS [14], ammonium adducts of H-PDMS exhibit very similar dissociation pattern regardless of the size of the precursor ion, as illustrated by the case of the 23-mer at m/z 1780 in Fig. 1.

Three product ion series could be observed and, in a first approach, were referred to according to Mayer's et al. notation [11]. Ions of the main series detected at m/z 207, m/z 281 and m/z 355 (annotated with black squares in Fig. 1) were noted $(R_n + 59)^+$, with $R = SiOC_2H_6$ (*i.e.*, a DMS unit, 74 Da) and $n = 2$–4 respectively. Despite collision energy was lowered, the largest homologues ever observed in this series were detected with quite low abundance at m/z 429 ($n = 5$) and m/z 503 ($n = 6$). Based on their m/z values, ions from the second ion series (annotated with black triangles in Fig. 1) were called $(R_n + 73)^+$, with $n = 1$–5, while the third series (annotated with black stars in Fig. 1) consists of $(R_{3-5} + 45)^+$ ions of very low abundance.

3.2. Primary product ions: release of NH_3 (and H_2)

As demonstrated in the case of CH_3-PDMS [14] and consistently with their odd m/z values, all ions observed in MS/MS spectra of H-PDMS ammonium adducts would actually arise from secondary

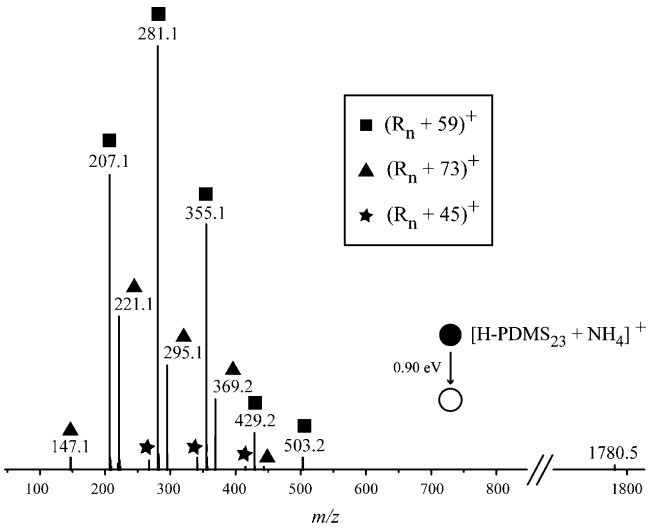

Fig. 1. ESI-MS/MS spectrum of the H-PDMS 23-mer ammonium adduct at *m/z* 1780.5, recorded at a 0.9 eV collision energy (center-of-mass frame).

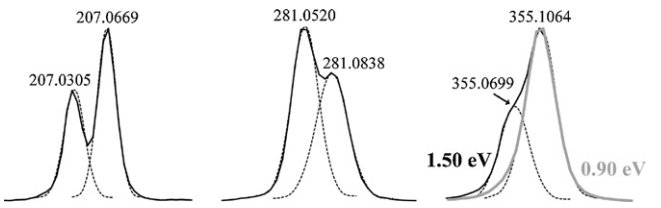

Fig. 3. Details of the ESI-MS/MS spectrum of the H-PDMS 23-mer ammonium adduct displayed in Fig. 1, showing isobaric ions are actually formed at *m/z* 207, *m/z* 281 and *m/z* 355.

Table 1
Accurate mass data and elemental composition assigned to the main product ions arising from the dissociation of *m/z* 1780.3.

Elemental composition	*n*	$(m/z)_{theo}$	$(m/z)_{exp}$	Error (ppm)
$(C_2H_6OSi)_nC_2H_7Si^+$	2	207.0687	207.0669	−8.7
	3	281.0875	281.0838	−13.2
	4	355.1063	355.1064	+0.3
$(C_2H_6OSi)_nCH_3OSi^+$	2	207.0324	207.0305	−9.2
	3	281.0511	281.0520	+3.2
	4	355.0699	355.0699	0

dissociation of product ions generated upon the release of ammonia (observed to occur from oligomer precursors with *n* up to 10) or formed after precursor ions have eliminated NH_3 and H_2, as evidenced from CID of the smallest size congeners ($n < 8$). Similarly to the release of ammonia and methane observed from small size CH_3-PDMS ammonium adducts, this 19 Da loss would proceed according to a concerted process, H_2 being formed upon protonation of a H termination while NH_3 still interacts via hydrogen bonds with oxygen atoms of the polymeric backbone. Energetic cost associated with the proposed concerted NH_3/H_2 losses was compared to the energy required for a sequential release of these two neutrals, using a 1-mer model (tetramethyldisiloxane, further noted TMDSO). Typical Transition State modelization allowed us to propose potential activation barrier for each pathway. As illustrated in Fig. 2, the concerted loss of NH_3 and H_2 would require a lower activation energy (82.8 kJ mol^{-1}) as compared to a total of 120.0 kJ mol^{-1} for a two step release. It should also be noted that, although numerous methyl groups were available, release of methane together with ammonia (as reported from CH_3-PDMS [14]) was not observed to occur from $[H\text{-PDMS} + NH_4]^+$. Theoretical calculations indeed indicate that loss of CH_4 did not efficiently compete with elimination of H_2, as shown by energy data associated with methane elimination, either from protonated TMDSO or in conjunction with ammonia from TMDSO ammonium adduct (Fig. 2).

3.3. Structure and formation of the main product ions (m/z 207, 281, 355)

A closest inspection of peak shape of the three main product ions at *m/z* 207, *m/z* 281 and *m/z* 355 indicates that these signals should not be assigned to a unique ionic form. Using the highest resolving power accessible with our oa-TOF mass analyzer, two distinct ions were shown to contribute to each signal, as illustrated in Fig. 3.

It should be noted here that the presence of a second ionic species at *m/z* 355 could only be evidenced while increasing the center-of-mass collision energy from 0.90 eV to 1.50 eV. Accurate mass measurements allowed elemental composition to be assigned for these six ions (Table 1). A $(C_2H_6OSi)_nC_2H_7Si^+$ general formula could be assigned to a first set of product ions while the second one would be of the form $(C_2H_6OSi)_nCH_3OSi^+$.

Based on our previous work on CH_3-PDMS [14], a cyclic structure consisting of n DMS units and containing one positively charged oxygen atom bound to a dimethylsilane pendant group (Scheme 1a) could be assigned to the $(C_2H_6OSi)_nC_2H_7Si^+$ product ions. A cycle

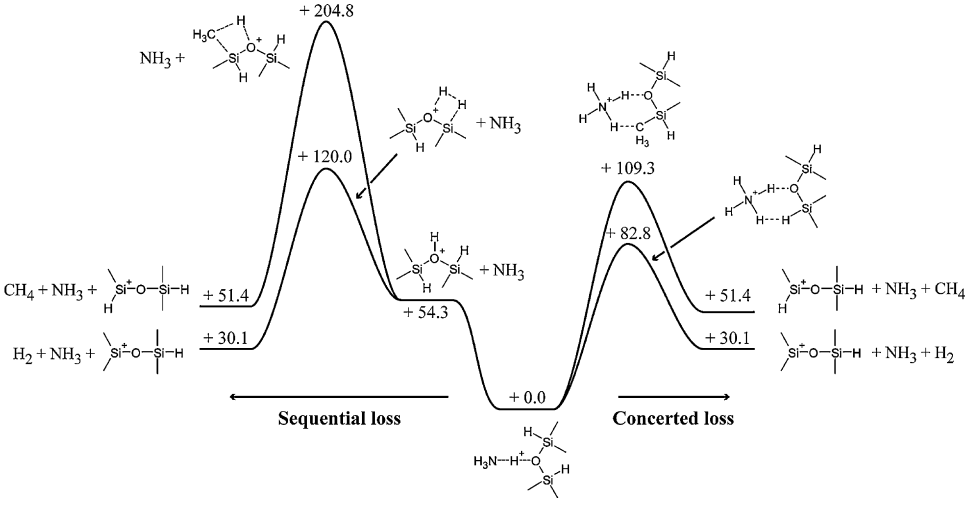

Fig. 2. Calculated potential energy surface for the release of ammonia + hydrogen and ammonia + methane from the ammonium adduct of a tetramethyldisiloxane model molecule, according to a sequential (left-hand side) or a concerted (right-hand side) process. Energies are given in kJ mol^{-1}.

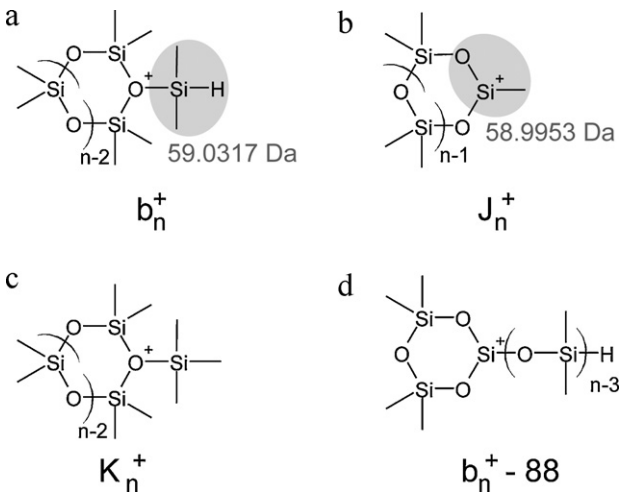

Scheme 1. Structures proposed for product ions observed in CID spectra of H-PDMS ammonium adducts: (a) b_n^+ ions with $(C_2H_6OSi)_nC_2H_7Si^+$ elemental composition and detected with n = 2–4 at m/z 207, m/z 281 and m/z 355, (b) J_n^+ ions with $(C_2H_6OSi)_nCH_3OSi^+$ elemental composition and detected with n = 2–4 at m/z 207, m/z 281 and m/z 355, (c) K_n^+ ions with $(C_2H_6OSi)_nC_3H_9Si^+$ elemental composition and detected with n = 2–4 at m/z 221, m/z 295 and m/z 369, and (d) b_n^+-88 ions with $(C_2H_6OSi)_nHOSi^+$ elemental composition and detected with n = 3–5 at m/z 267, m/z 341 and m/z 415.

built from n intact DMS units and one with a positively charged Si atom lacking a methyl group (Scheme 1b) was proposed to account for the $(C_2H_6OSi)_nCH_3OSi^+$ elemental composition.

To distinguish these two ion series, the general nomenclature recently proposed by Wesdemiotis et al. [1] was adopted here. Accordingly $(C_2H_6OSi)_nC_2H_7Si^+$ product ions (Scheme 1a) should be noted b_n^+: the letter b indicates these fragments retain the initiating chain end (actually, H-PDMS has a symmetrical structure and indistinguishable end-groups and in such cases, letters from the beginning of the alphabet should be considered) and they arise from cleavage of the second type of bonds encountered in the PDMS polymeric backbone. A superscripted plus sign is added since they do no longer contain the adducted ammonium cation, and the subscripted n value gives the number of complete or partial repeat units contained in the fragment. In contrast, in the structure proposed for $(C_2H_6OSi)_nCH_3OSi^+$ product ions (Scheme 1b), both original end groups are missing: as a result, these internal fragments arising from secondary dissociations were called J_n^+.

As in the case of CH_3-PDMS, geometrical optimizations performed for b_{2-4}^+ product ions systematically lead to cyclic structures containing as many DMS units as possible, with a dimethylsilyl substituent on a positively charged oxygen (Form I). However, in the case of H-PDMS, iso-energetic pseudo-cyclic structures could also be proposed, with a positively charged silicon atom stabilized by non-covalent bond with the residual hydride end-group (Form II). Both conformations are exemplified for b_2^+ in Table 2, together with calculated B3LYP/6-311g(2d,p) energies obtained for b_{2-4}^+ product ions.

While b_{2-4}^+ product ions were always produced in similar relative abundance during CID of the largest precursor ions, MS/MS spectra obtained for the smallest oligomers (n < 10) displayed slightly different peak patterns depending on the polymerization degree of the dissociating precursor. More particularly, the highest peak was obtained for b_4^+ at m/z 355 in the cases of 4-mer (m/z 374) and 7-mer (m/z 596), for b_3^+ at m/z 281 during MS/MS of 6-mer (m/z 522) and 9-mer (m/z 744), and for b_2^+ at m/z 207 upon CID of 5-mer (m/z 448) and 8-mer (m/z 670). In other words, the most abundant b_n^+ ion was always obtained after the precursor ion has eliminated NH_3 and H_2, as well as a 222p Da neutral, with p = 0 for the 4-mer, p = 1 for the 5- to the 7-mers, and p = 2 for the 8-mer and the 9-mer. Since geometrical optimizations have shown that lowest energy conformations correspond to cyclic structures involving DMS units [14], this 222 (=3 × 74) Da neutral could be seen as a cycle composed of three DMS units, further noted D_3, according to the traditional silicone nomenclature. Accordingly, two different dissociation pathways should be considered to account for the formation of b_n^+ ions, depending on the size of dissociating precursors. In the smallest oligomers (n < 10), the adducted ammonium cation would interact with a chain end, allowing a concerted elimination of NH_3 and H_2 and the formation of a product ion in which the positive charge is hold by a terminal Si atom. A subsequent 1,6-electron transfer from a lone pair of an O atom to this charged Si atom would be induced by a backbiting reaction, as depicted in Scheme 2a for the 5-mer precursor ion. This reaction would give rise to the release of the D_3 neutral (222 Da) and the formation of a cyclic b_n^+ product, which size varies as a function of the initial number of DMS units in the polymeric backbone.

For largest oligomers, it was thus postulated that the adducted ammonium cation would interact to a lesser extent with the terminal H, lowering the possibility for a concerted loss of NH_3/H_2. In contrast, elimination of a sole ammonia molecule would be favored, producing a protonated oligomer which would further dissociate according to the pathway depicted in Scheme 2b. This alternative mechanism would proceed via the cleavage of different Si–O$^+$(H) bonds in the polymeric backbone depending on the protonated oxygen location, leading to the production of b_n^+ product ions upon release of neutral monohydroxy linear PDMS in a backbiting process. Depending on their size, these product ions would further dissociate via elimination of cyclic siloxane neutral (D_n) to ultimately lead to the formation of the most stable b_{2-4}^+ congeners of this series.

To account for the preferential release of a 222 Da neutral in the second step of Scheme 2a, energetic costs associated with the elimination of different D_i molecules were calculated, starting from different precursor ions. Despite the large size of the considered precursor ions (b_5^+ at m/z 429, b_6^+ at m/z 503 and b_7^+ at m/z 577), conformational space exploration was dramatically reduced by considering the favorable cyclic structure previously proposed for the smallest b_n^+ product ions. Dimethylsiloxane units were typically added step by step to the dimethyl substituent from the eight-membered ring structure of b_4^+ so as to produce a linear backbone. Chain fold was then carefully carried out by optimizing favorable intramolecular interactions between oxygen atoms from the linear part and methyl groups from the cyclic part. Such a cyclolinear structure was found to be energetically favored as compared to the equivalent macrocyclic shape. Energies calculated in the cases of the 5-, 6- and 7-mers show that the release of a D_3 neutral is always energetically favored, with an amount of energy of 53.2, 32.2 and 46.3 kJ mol^{-1}, respectively (Fig. 4). These calculations also indicate that elimination of larger D_i cycles seems to compete more efficiently with the release of D_3 as the size of precursor increases. For example, the energy cost associated with elimination of D_3 from the 7-mer (46.3 kJ mol^{-1}) is very close to the value calculated for the release of D_4 (48.0 kJ mol^{-1}). Interestingly, energy cost associated with a 444 Da neutral loss could be dramatically reduced by considering elimination of two D_3 cycles rather than one D_6 ring (from 212.0 to 150.1 kJ mol^{-1} in the case of the 6-mer precursor ion in Fig. 4).

Finally, J_{2-4}^+ product ions ($(C_2H_6OSi)_nCH_3OSi^+$ in Scheme 1b) would respectively be formed upon loss of a trimethylsilane neutral (74 Da) from b_{3-5}^+ ions, considering a methyl transfer from a Si atom involved in DMS ring to the neighbored dimethylsilyl pendant group [1,11]. A similar process was observed to allow tetramethylsilane molecule to be released in the case of CH_3-PDMS [14].

Table 2
Isoenergetic conformations of b_n^+ product ions at *m/z* 207, *m/z* 281 and *m/z* 355 evaluated by B3LYP/6-311g(2d,p) optimizations. Both structures are exemplified for b_2^+ at *m/z* 207. ΔE refers to form II as compared to form I.

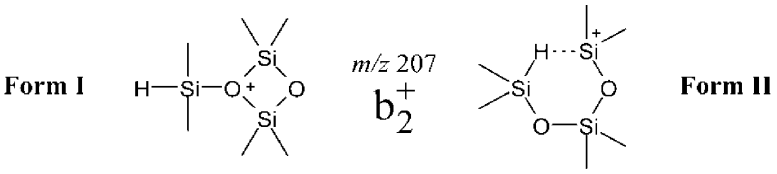

	Calculated energy (Ha)		ΔE (kJ mol^{-1})
	Form I	Form II	
m/z 207	−1259.090732	−1259.090989	−0.7
m/z 281	−1703.794242	−1703.792542	+4.5
m/z 355	−2148.491049	−2148.489902	+3.0

3.4. Structure and formation of secondary product ions

Apart from the main ion series, two other product ion distributions could be observed during CID of H-PDMS ammonium adducts. Ions detected at *m/z* 221, *m/z* 295 and *m/z* 369 (annotated with black triangles in Fig. 1) could be described as $(C_2H_6OSi)_nC_3H_9Si^+$ with $n = 2–4$,, respectively. This series is completed by congeners with $n = 1$ and $n = 5$ of very low abundance. According to the structure proposed for these product ions (Scheme 1c), they were called K_n^+. In addition, very low intensity peaks were observed at *m/z* 267, *m/z* 341 and *m/z* 415 (indicated by black stars in Fig. 1). Based on accurate mass data suggesting an elemental composition such as $(C_2H_6OSi)_nHOSi^+$ with $n = 3–5$ as well as MS^3 experiments (data not shown), these product ions arising from secondary dissociation of b_n^+ were called b_n^+-88 (Scheme 1d). Mechanisms proposed for the formation of these two series are illustrated in Scheme 3, starting from the b_6^+ intermediate to generate K_2^+ at *m/z* 221 and b_6^+-88 at *m/z* 415. A 1,7-transfer of a methyl group from the pendant chain in b_6^+ (pathway 1 in Scheme 3) would induce opening of the six-membered ring. Then, a concerted electron transfer would allow K_2^+ to be produced upon release of a 282 Da neutral. Alternatively, formation of b_6^+-88 would proceed via two methyl group migrations. The first one would be a 1,3-transfer from the pendant chain, as depicted by pathway 2 in Scheme 3, while the second one (a 1,7-transfer) would allow tetramethylsilane (88 Da) to be eliminated as a neutral.

3.5. Comparison of CID behaviors: H-PDMS vs. CH_3-PDMS

When comparing dissociation patterns of H-PDMS and CH_3-PDMS ammonium adducts, MS/MS spectra were shown to contain the same two series of peaks, regardless of the nature of polymer terminations. Major signals were obtained for $b_{2–4}^+$ product ions, respectively detected at *m/z* 207, *m/z* 281 and *m/z* 355 for H-PDMS and at *m/z* 221, *m/z* 295 and *m/z* 369 for CH_3-PDMS. A lower abundance secondary peak series is composed of $K_{3–5}^+$ product ions, observed at *m/z* 221, *m/z* 295 and *m/z* 369 for H-PDMS and at *m/z* 207, *m/z* 281 and *m/z* 355 for CH_3-PDMS, respectively. As a result, these two synthetic polymers can be distinguished in MS/MS based on relative abundance of these two ion sets. Another noticeable difference between CID of these two polymeric species is the relative abundance of product ions within each series, when arising from the smallest precursor ions. While b_n^+ ions were produced with similar relative abundance regardless of the size of CH_3-PDMS molecules, MS/MS spectra obtained for H-PDMS ammonium adducts displayed different b_n^+ peak patterns depending on the polymerization degree of the dissociating precursor. This last result was explained by preferential elimination of D_3 neutrals

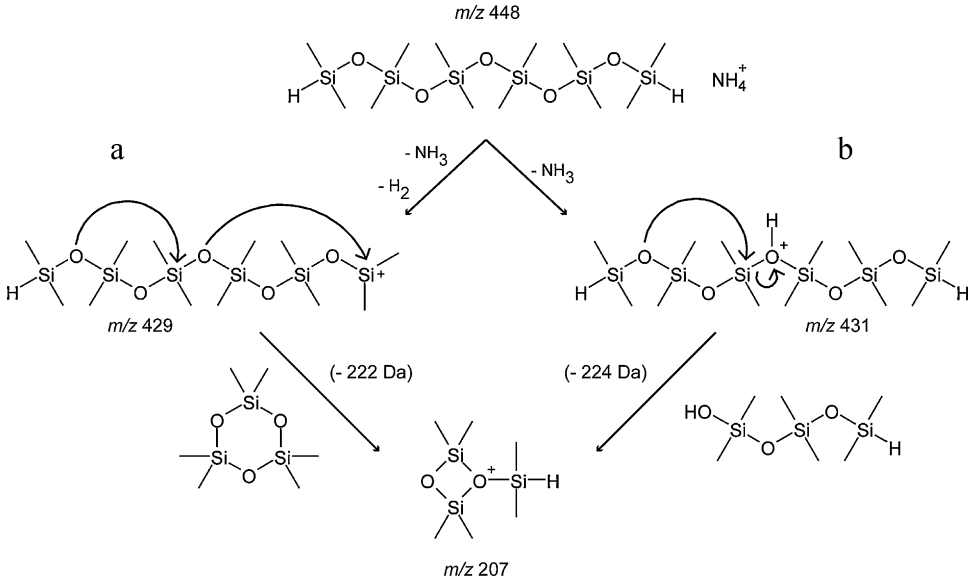

Scheme 2. Proposed mechanisms for the formation of b_n^+ product ions from ammonium adduct of (a) small and (b) large H-PDMS oligomers.

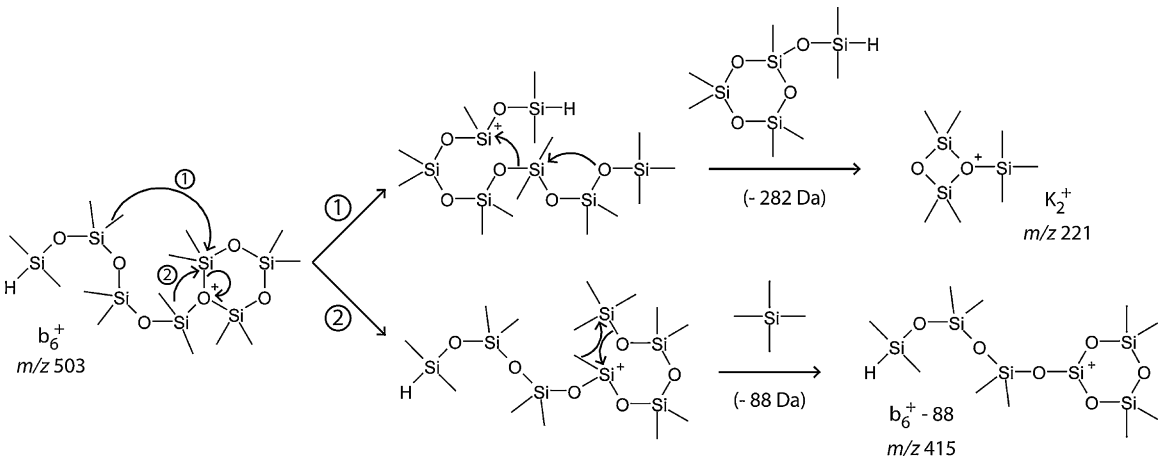

Scheme 3. Proposed mechanisms to account for the formation of secondary product ions K_n^+ and b_n^+-88 from b_n^+.

(222 Da) once $[H\text{-}PDMS + NH_4]^+$ has eliminated NH_3 and H_2 in a concerted manner, *i.e.*, when the positive charge is carried by a terminal Si atom. This would suggest a greater propensity of the terminal H atom to interact with protons of the ammonium cation, as compared to CH_3.

This feature can be illustrated by measuring the degree of similarity between MS/MS spectra of consecutive oligomers within PDMS distribution. Since b_{2-5}^+ and K_{2-5}^+ were found to be diagnostic product ions for both CH_3-PDMS and H-PDMS small oligomers, relative abundances of these $i = 8$ ions were measured in CID spectra of the n- and $(n+1)$-mer ammonium adducts, and respectively noted ${}^iI_n$ and ${}^iI_{n+1}$. The degree of similarity, as expressed by the relative Euclidian distance, between MS/MS spectra of n- and $(n+1)$-mer is then calculated according to:

$$d_{n+1/n}^{\text{relative}} = \frac{\sqrt{\sum_i {}^iI_{n+1} - {}^iI_n|^2}}{d_{\max}}$$

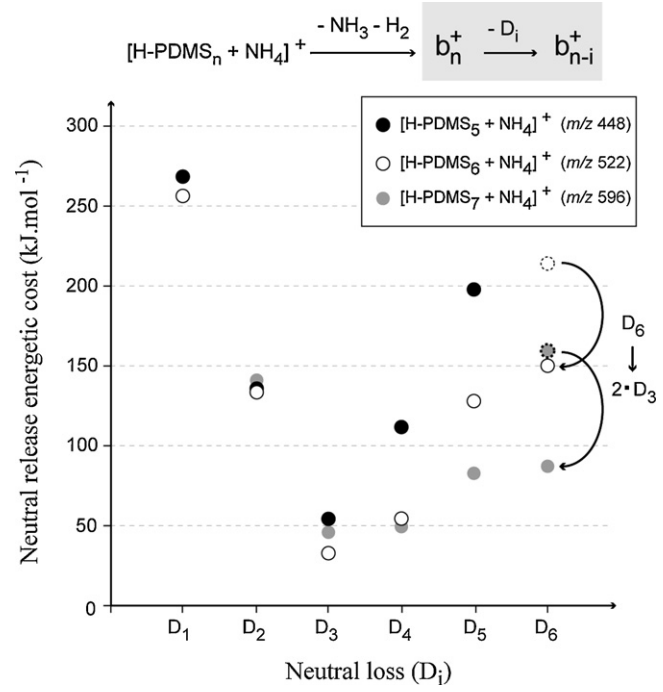

Fig. 4. Calculated energy for the release of D_{1-6} neutrals, proposed to occur after a concerted elimination of $NH_3 + H_2$ from the smallest ($n < 10$) H-PDMS oligomer ammonium adducts.

where $d_{\max}$ is the maximum calculated distance, used as a normalization coefficient.

Plotting relative Euclidian distances calculated for all oligomers as a function of their polymerization degree (Fig. 5) allows the repeatability of MS/MS patterns to be evaluated for ammonium adducts of H- and CH_3-PDMS as the size of the chain increases. Data presented in Fig. 5 allow the slightly different CID behavior between H- and CH_3-PDMS to be better emphasized. While the same MS/MS spectra were observed for any CH_3-PDMS ammonium adducts from the 9-mer, as indicated by low and constant values of the relative Euclidian distance measured from $n = 9$, repeatability of the CID pattern is really obtained from $n = 15$ in the case of H-PDMS. As previously discussed, we assumed that a high degree of similarity between MS/MS spectra of consecutive oligomers would be reached once the end-group would no longer be involved in dissociative pathway. For CH_3-PDMS, a lower degree of similarity (*i.e.*, a higher relative Euclidian distance) is indeed measured between the 7- and the 8-mers ($d = 0.30$ at $n = 7$), than between the 8- and the 9-mers ($d = 0.10$ at $n = 8$), consistently with MS/MS data showing methyl end-groups were involved in dissociation pathways up to the 7-mer. In the case of H-PDMS, results presented in Fig. 5 would indicate that the release of NH_3 and H_2, although only evidenced up to the 7-mer, would actually proceed up to the 15-mer. This would reveal a much higher reactivity of the terminal H atoms towards ammonium protons as compared to the methyl groups.

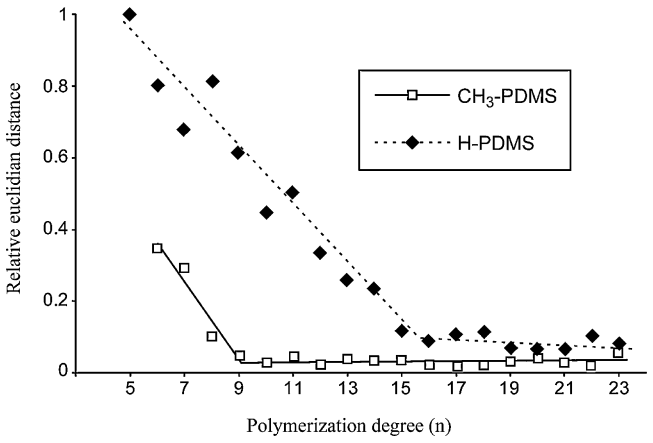

Fig. 5. Relative Euclidian distance between consecutive MS/MS spectra of H- and CH_3-PDMS ammonium adducts as a function of polymerization degree.

4. Conclusion

Similarly to trimethylsilyl-terminated PDMS, ammonium adducts of α,ω-dihydride linear PDMS were shown to always generate the same three major product ions upon CID, regardless of the size of the precursor ion. Particularly stable cyclic structures calculated for these three main ions as well as for released neutrals in proposed dissociation mechanisms could account for this peculiar MS/MS behavior. Additional signals in CID spectra of all oligomers were shown to be secondary ions generated upon dissociation of the main product ions. Perfect similarity of MS/MS spectra as the size of the polymeric chain increases is however only reached once the end-groups are no longer involved in the primary dissociative pathway, consisting of the release of NH_3 and H_2. This feature could clearly be evidenced by measuring Euclidian relative distance between CID spectra of consecutive precursor ions, showing a much higher reactivity of hydride terminations towards the adducted ammonium cation, as compared to methyl end-groups.

Acknowledgments

L. Charles acknowledges support from Spectropole, the Analytical Facility of Aix-Marseille University, by allowing a special access to the instruments purchased with European Funding (FEDER OBJ2142-3341). Financial support by the Luxembourg Research Funding Association FNR (Fond National de la Recherche) is also gratefully acknowledged.

Appendix A. Supplementary data

Supplementary data associated with this article can be found, in the online version, at doi:10.1016/j.ijms.2011.06.020.

References

[1] C. Wesdemiotis, N. Solak, M.J. Polce, D.E. Dabney, K. Chaicharoen, B.C. Katzenmeyer, Fragmentation pathways of polymer ions, Mass Spectrom. Rev. 30 (2011) 523–559.
[2] K. Matyjaszewski, Controlled/Living Radical Polymerization, American Chemical Society, Washington, DC, 2000, Vol. Series 786.
[3] M. Mazarin, M. Girod, S. Viel, T.N.T. Phan, S.R.A. Marque, S. Humbel, L. Charles, Role of the adducted cation in the release of nitroxide end group of controlled polymer in mass spectrometry, Macromolecules 42 (2009) 1849–1859.
[4] C.J. Hawker, A.W. Bosman, E. Harth, New polymer synthesis by nitroxide mediated living radical polymerizations, Chem. Rev. 101 (2001) 3661–3688.
[5] R.P. Lattimer, Tandem mass-spectrometry of lithium-attachment ions from polyglycols, J. Am. Soc. Mass Spectrom. 3 (1992) 225–234.
[6] R.P. Lattimer, Tandem mass-spectrometry of poly(ethylene glycol) lithium-attachment ions, J. Am. Soc. Mass Spectrom. 5 (1994) 1072–1080.
[7] T.L. Selby, C. Wesdemiotis, R.P. Lattimer, Dissociation characteristics of M + X (+) Ions (X = H, Li, K) from linear and cyclic polyglycols, J. Am. Soc. Mass Spectrom. 5 (1994) 1081–1092.
[8] S. Okuno, M. Kiuchi, R. Arakawa, Structural characterization of polyethers using matrix-assisted laser desorption/ionization quadrupole ion trap time-of-flight mass spectrometry, Eur. J. Mass Spectrom. 12 (2006) 181–187.
[9] J.P. Williams, G.R. Hilton, K. Thalassinos, A.T. Jackson, J.H. Scrivens, The rapid characterisation of poly(ethylene glycol) oligomers using desorption electrospray ionisation tandem mass spectrometry combined with novel product ion peak assignment software, Rapid Commun. Mass Spectrom. 21 (2007) 1693–1704.
[10] M. Girod, Y. Carissan, S. Humbel, L. Charles, Tandem mass spectrometry of doubly charged poly(ethylene oxide) oligomers produced by electrospray ionization, Int. J. Mass Spectrom. 272 (2008) 1–11.
[11] J. Renaud, A.M. Alhazmi, P.M. Mayer, Comparing the fragmentation chemistry of gas-phase adducts of poly(dimethylsiloxane) oligomers with metal and organic ions, Can. J. Chem. 87 (2009) 453–459.
[12] H. Chen, Endgroup-assisted siloxane bond cleavage in the gas phase, J. Am. Soc. Mass Spectrom. 14 (2003) 1039–1048.
[13] A.M. Leigh, P. Wang, M.J. Polce, C. Wesdemiotis, Tandem mass spectrometry of poly(siloxane)s, in: 53rd ASMS Conference on Mass Spectrometry and Allied Topics, June 5–9, San Antonio, Texas, 2005.
[14] T. Fouquet, S. Humbel, L. Charles, Tandem mass spectrometry of trimethylsilyl-terminated poly(dimethylsiloxane) ammonium adducts generated by electrospray ionization, J. Am. Soc. Mass Spectrom. 22 (2011) 649–658.
[15] L. Charles, Influence of internal standard charge state on the accuracy of mass measurements in orthogonal acceleration—time of flight mass spectrometers, Rapid Commun. Mass Spectrom. 22 (2008) 151–155.
[16] M.J. Frisch, G.W. Trucks, H.B. Schlegel, G.E. Scuseria, M.A. Robb, J.R. Cheeseman, J.A. Montgomery Jr, T. Vreven, K.N. Kudin, J.C. Burant, J.M. Millam, S.S. Iyengar, J. Tomasi, V. Barone, B. Mennucci, M. Cossi, G. Scalmani, N. Rega, G.A. Petersson, H. Nakatsuji, M. Hada, M. Ehara, K. Toyota, R. Fukuda, J. Hasegawa, M. Ishida, T. Nakajima, Y. Honda, O. Kitao, H. Nakai, M. Klene, X. Li, J.E. Knox, H.P. Hratchian, J.B. Cross, C. Adamo, J. Jaramillo, R. Gomperts, R.E. Stratmann, O. Yazyev, A.J. Austin, R. Cammi, C. Pomelli, J.W. Ochterski, P.Y. Ayala, K. Morokuma, G.A. Voth, P. Salvador, J.J. Dannenberg, V.G. Zakrzewski, S. Dapprich, A.D. Daniels, M.C. Strain, O. Farkas, D.K. Malick, A.D. Rabuck, K. Raghavachari, J.B. Foresman, J.V. Ortiz, Q. Cui, A.G. Baboul, S. Clifford, J. Ciolowski, B.B. Stefanov, G. Liu, A. Liashenko, P. Piskorz, I. Komaromi, R.L. Martin, D.J. Fox, T. Keith, M.A. Al-Laham, C.Y. Peng, A. Nanayakkara, M. Challacombe, P.M.W. Gill, B. Johnson, W. Chen, M.W. Wong, C. Gonzalez, J.A. Pople, Gaussian 03, C.02; Wallingford, 2004.
[17] A.D. Becke, Density-functional thermochemistry. 3. The role of exact exchange, J. Chem. Phys. 98 (1993) 5648–5652.
[18] C.T. Lee, W.T. Yang, R.G. Parr, Development of the Colle-Salvetti correlation-energy formula into a functional of the electron-density, Phys. Rev. B 37 (1988) 785–789.
[19] F. De Proft, F. Tielens, P. Geerlings, Performance and basis set dependence of density functional theory dipole and quadrupole moments, J. Mol. Struct. THEOCHEM 506 (2000) 1–8.
[20] G.T. de Jong, F.M. Bickelhaupt, Oxidative addition of the fluoromethane C–F bond to Pd. An *ab initio* benchmark and DFT validation study, J. Phys. Chem. A 109 (2005) 9685–9699.
[21] G.T. de Jong, D.P. Geerke, A. Diefenbach, F.M. Bickelhaupt, DFT benchmark study for the oxidative addition of CH_4 to Pd. Performance of various density functionals, Chem. Phys. 313 (2005) 261–270.
[22] R. Krishnan, J.S. Binkley, R. Seeger, J.A. Pople, Self-consistent molecular-orbital methods. 20. Basis set for correlated wave-functions, J. Chem. Phys. 72 (1980) 650–654.
[23] J.P. Blaudeau, M.P. McGrath, L.A. Curtiss, L. Radom, Extension of Gaussian-2 (G2) theory to molecules containing third-row atoms K and Ca, J. Chem. Phys. 107 (1997) 5016–5021.
[24] J.B. Foresman, A. Frisch, Exploring Chemistry with Electronic Structure Methods, second ed., Gaussian Inc., Pittsburgh, 1995.
[25] Y. Kawakami, Y. Li, Y. Liu, M. Seino, C. Pakjamsai, M. Oishi, Y.H. Cho, I. Imae, Control of molecular weight, stereochemistry and higher order structure of siloxane-containing polymers and their functional design, Macromol. Res. 12 (2004) 156–171.